



Semnan University



# Numerical investigation of heat transfer in a sintered porous fin in a channel flow with the aim of material determination

Mehrdad Mesgarpour<sup>a</sup>, Ali Heydari<sup>\*b</sup>, Seyfolah Saedodin<sup>c</sup>

<sup>a</sup> Department of Mechanical Engineering, Semnan Branch, Islamic Azad University, Semnan, Iran.

<sup>b</sup> Energy and Sustainable Development Research Center, Semnan Branch, Islamic Azad University, Semnan, Iran.

<sup>c</sup> Department of Mechanical Engineering, Semnan University, Semnan, Iran

## PAPER INFO

### Paper history:

Received: 2018-08-05

Received: 2018-12-17

Accepted: 2018-12-29

### Keywords:

Engineered porous fin Sintering;  
Nusselt number

## ABSTRACT

Extended surfaces are one of the most important approaches to increase the heat transfer rate. According to the Fourier law, the heat transfer increases by increasing the contact surface of the body and fluid. In this study, the effect of heat transfer has been investigated on two sets of engineered porous fins, in which the balls with different materials are sintered together. The fluid flow through the channel was considered incompressible, steady, and three-dimensional. Furthermore, fins made up of copper, aluminum and steel balls with 0.6 and 1.7 mm diameters in single-row, two-rows modes were studied, and the heat transfer and pressure drop through these fins were checked. Moreover, the surface and volume analyses of the rigid and porous fins were provided. In addition, the effect of diameter and material of the balls on the temperature distribution and heat transfer coefficient has been examined in two cases of constant flux and constant temperature at the base. The results indicate that the steel fin has a different heat transfer behavior compared to other fins. The suitable material for the constant temperature and constant flux are copper and aluminum, respectively. Also, it was found that the utilization of this type of connection would decrease the volume of the fin about 39% and increase the surrounding surface by 37%.

DOI: 10.22075/jhmtr.2018.15442.1215

© 2019 Published by Semnan University Press. All rights reserved.

## 1. Introduction

Extensive surfaces are the most important strategy to increase the heat transfer rate from the surface of bodies. In many cases, due to different reasons, it is not possible to use other methods for increasing heat transfer. The need for utilization of extended surfaces is seen in many engineering devices and equipment. There are various types of extended surfaces used in a specific position, depending on the characteristics of each item. Heat in the fin is transferred based on the conduction type which leads to heat transfers along the solid body of the fin from the base. Then, the heat is dissipated by convection and radiation through the surface boundaries of the fin. The conductive heat transfer is one of the most well-known principles of heat transfer [1]. Researchers have been looking for ways to increase the performance and

efficiency of heat transfer in the fins for many years. Changing the shape and material could be considered as the ways to increase the performance of the fin. In 1993, Bejan and Morega [2] examined the thermal resistance of the porous fins. The results show that the lowest thermal resistance in the porous fins row is approximately half of the least thermal resistance of the heat sink with continuous fins and fully developed flow. Wirtz et al. [3] investigated the cooling effect on a porous fin. The results indicate that if a spherical model is utilized in a porous media matrix, the pressure drop reaches its minimum value for a cooling flow. In a numerical investigation, Jeng and Tzeng [4] evaluated the heat transfer in a porous fin. According to the results, in the low Reynolds numbers, the highest Nusselt number occurs at the stagnation point. This point goes towards the downstream as the Reynolds

\*Corresponding Author: A. Heydari, Energy and Sustainable Development Research Center, Semnan Branch, Islamic Azad University, Semnan, Iran.  
Email: a.heydari@semnaniau.ac.ir.

number increases. Ma et al. [5] developed a spectral element method (SEM) to study the conductive, convective, and radiative heat transfer in moving porous fins of trapezoidal, convex parabolic and concave parabolic profiles. They indicated that SEM could provide good accuracy. In another work, Ma et al. [6] also used least square spectral collocation method (LSSCM) to predict the temperature distribution and heat transfer efficiency of moving the porous plate. They showed that this model is of high accuracy and good flexibility to simulate the nonlinear heat transfer in moving the porous plate. They also presented spectral collocation method (SCM) to predict the thermal performance of convective–radiative porous fin [7]. They verified the accuracy of the SCM model by comparing with numerical results. Hamadan and Moh'd [8] studied the effect of the porous fin in a channel with parallel plates. The results showed that the highest Nusselt number in this problem corresponds to the maximum produced pressure of the pump. It was also indicated that for a porous medium placed in this channel, lower pressure of the inlet pump to the solid fin is required for increasing the thermal efficiency. The various applications of conventional and porous fins have led many researchers to specific areas of this field. With the advancement of electronic systems and the use of integrated circuits in them, heating issues and microchannel heat sinks are introduced. Chuan et al. [9] investigated the fluid flow and heat transfer in a microchannel heat sink based on the porous fin design concept. As compared with that of the conventional heat sink, they showed that the pressure drop of the new design would be reduced by 43.0% to 47.9% at various coolant flow rates. However, the thermal resistance increases only about 5%. Lu et al. [10] applied wavy porous fins as a new scheme for reducing pressure drop and thermal resistance simultaneously in microchannel heat sinks. They examined the new concept for various micro-channel heat sink designs with different wavy amplitude, wavelength, and channel width and height. One of the latest works was done by Ong [11]. He studied the effect of cooling on the semiconductor chips and introduced new mechanisms such as surface evaporation and usage of thermoelectric. He also evaluated the effectiveness of the proposed mechanisms by numerical analysis using software and manual solution. Due to the conjugated nature of heat transfer in the fin, especially in natural convection, the gravitational effects have great effects. A variation in the temperature of the fin occurs based on the growth of the thermal boundary layer. This issue was the basis for Lindstedt and Karvinen's research [12]. They provided a suitable explanation for the relationship between the thermal conductivity of the fin and the flow flux from the fin to the surrounding fluid by solving a partial differential equation for the flow of fluid through the fin. One of the methods for optimizing the fins is to study the rate of entropy generation rate. Bijan suggested that with reducing the entropy generation rates of the system, the performance could be improved [13]. In 2016, Chen [14]

used this method to optimize needle fins. He investigated the optimal geometric specifications by considering the variable dimensions for the fin. The results showed that the most important parameter in optimization is the aspect ratio of the cross-section to the length. Furthermore, he figured that the heat distribution changes with an increase in the ratio of the diameter to the height. In recent work, Heydari et al. [15] numerically investigated the heat transfer and fluid flow around a bundle of the tapered porous fin. They showed that in laminar flow, the Nusselt number of the flow with the porous medium is 33% higher, and the pressure drop is 9.35% lower than the rigid one with the same conditions. They also presented an equation for Nusselt number based on the Reynolds number. New structures generally named as “engineered porous medium” have been created to eliminate the mentioned problems and precise design of the porous medium. In these porous structures, the constituent particles would be designed and manufactured according to a desired purpose and application. There are several ways to produce these mediums. The most common of them is the sintering process. In this method, the powder with a ball-shaped structure is produced from the base metal and would be converted into a solid piece under special pressure and temperature. Jiang et al. [16, 17] experimentally and numerically investigated the effects of fluid velocity, particle diameter, type of porous media (sintered or non-sintered), and fluid properties on convection heat transfer in a porous plate channel. They showed that the convection heat transfer of the sintered porous plate channel was more intense than in the non-sintered one due to the reduced thermal contact resistance and the reduced porosity, especially for air. Also, their results indicated that the effective thermal conductivity of the sintered porous media was found to be much higher than for non-sintered one due to the improved thermal contact caused by the sintering process. Later, Jiang and Lu [18] numerically analyzed the sintered balls in a channel to investigate heat transfer in such balls. They observed that, with reducing the size of the spheres, heat transfer increases. In a recent work, an investigation about the connection type of balls for an engineered porous fin was done by Mesgarpour et al. [19]. It was indicated that the six-contact model (diagonal connection type) has more porosity than the four-contact model (vertical connection type) in reference cube by 29.45%. It was further found that the six-contact model tends to increase convective heat transfer by 33%. Reviewing the conducted studies on porous fins, it has become clear that a few works have been done on the engineered porous fins, and there is a lack of adequate research in this field.

Therefore, in the present work, a porous fin is designed by rows of stuck balls together, in which the diameter and material of the balls can be changed. Also, its effect on the heat transfer coefficient and temperature distribution of the fin surface for two boundary conditions of constant temperature and constant heat flux at the base is investigated.

## 2. Governing equations for rigid and porous fins

For the accurate description of the heat transfer principles and the temperature distribution in a porous body, the following items should be checked:

- Equation of energy (simple form)
- Equation of energy (complex and extended form)
- The equation of continuity
- Temperature distribution model

Evaluating the above issues could lead to a deep understanding of heat transfer mechanisms in porous bodies. The main mechanical equations include the conservation equations of energy and mass that are the basis for the thermal behavior of the fluid. In the porous body, as in other bodies, these equations are established. For a porous body, it is necessary to introduce the fluid moving environment in a porosity, which is referred to as representative elementary volume (REV). In order to establish continuity in the environment, it is considered that REV is a continuous and unit environment in which all the equations are established.

Porosity is the most important feature of the porous body, which is a physical property. Porosity measurements are conducted in a variety of ways [20-22]. The governing equation of a non-porous fin considering the radiation and convection is as follows:

$$\frac{d^2T}{dx^2} - \frac{hp}{KA_c}(T_s - T_\infty) - \frac{\sigma \epsilon p}{KA_c}(T_s^4 - T_\infty^4) = 0 \quad (1)$$

In the above relation,  $T_s$  is the fin surface temperature,  $K$  is the thermal conductivity,  $\sigma$  is the Stefan Boltzmann constant,  $P$  is the fin perimeter, and  $A_c$  is the cross section area of the fin. Giving the boundary conditions, the equation is expanded as follows.

$$\begin{aligned} T_{i+1} + T_{i-1} - \left(2 - \frac{hp\Delta x^2}{KA_c}\right)T_i + \left(\frac{\sigma \epsilon p\Delta x^2}{KA_c}\right)T_i^4 - \left(\frac{hp\Delta x^2}{KA_c}\right)T_\infty + \left(\frac{\sigma \epsilon p\Delta x^2}{KA_c}\right)T_\infty^4 &= 0 \\ T_{i+1} + T_{i-1} - \left(2 - \frac{hp\Delta x^2}{KA_c}\right)T_i + \left(\frac{\sigma \epsilon p\Delta x^2}{KA_c}\right)T_i^4 - \left(\frac{hp\Delta x^2}{KA_c}\right)T_\infty + \left(\frac{\sigma \epsilon p\Delta x^2}{KA_c}\right)T_\infty^4 &= 0 \end{aligned} \quad (2)$$

It should be noted that in the present work, the geometry of the porous medium was modeled directly considering the joined rigid balls, and flow analysis between the balls was also performed without activating Darcy and Dullien correlations in NS equations and applying their assumptions. The conservation equations of mass, momentum, and energy for this problem were applied in the common form. Because the porosity was created by designing the pattern and sorting the spheres which the solid body and the fluid region are completely delineated. In addition, the viscosity and inertial resistance of the porous medium would be calculated automatically by modeling the fluid flow through the balls. Therefore, it is not necessary to apply porosity correlations in the governing equations. The thermal conduction equation in the solid and rigid parts of the fin is:

$$\nabla \cdot (K_s \nabla T_s) = 0 \quad (3)$$

In the presence of the temperature gradient, the heat transfer occurs. The conservation equations of mass, momentum, and energy for this problem are:

$$\begin{aligned} \nabla \cdot (\rho U U) &= -\nabla P + \nabla \cdot \left( \mu \left( \nabla U - \frac{2}{3} \nabla \cdot U I \right) \right) \\ \nabla \cdot (\rho U H) &= \nabla \cdot (K_f \nabla T_f) \\ \nabla \cdot (\rho U) &= 0 \end{aligned} \quad (4)$$

in which,  $U$  is the fluid velocity,  $\rho$  is the fluid density,  $\mu$  is the fluid viscosity,  $H$  is the fluid enthalpy, and  $T$  is the fluid temperature. Also, in the momentum equation,  $I$  is equal to the unit tensor. Since the  $k-\omega$  model is used in this work, the related relations must also be presented [23]:

$$\begin{aligned} \frac{\partial}{\partial x_i} (\rho k u_i) &= \frac{\partial}{\partial x_j} \left( \left( \mu + \frac{\mu_t}{\sigma_k} \right) \frac{\partial k}{\partial x_j} \right) - \rho u_i' u_j' \frac{\partial u_j}{\partial x_i} - \rho \beta^* f_{\beta^*} \cdot k \omega \\ \frac{\partial}{\partial x_i} (\rho \omega u_i) &= \frac{\partial}{\partial x_j} \left( \left( \mu + \frac{\mu_t}{\sigma_k} \right) \frac{\partial \omega}{\partial x_j} \right) - \alpha \frac{\omega}{k} \rho u_i' u_j' \frac{\partial u_j}{\partial x_i} - \rho \beta f_{\beta} \cdot \omega^2 \end{aligned} \quad (5)$$

The constant coefficients of these two equations are provided in the reference [23]. In this case, the boundary conditions are very important in the interface between the fluid and solid. Consequently:

$$\begin{aligned} k_f \nabla T(f|i) &= k_s \nabla T(s|i) \\ T(f|i) &= T(s|i) \end{aligned} \quad (6)$$

Thermal efficiency and effectiveness of the fin can be calculated from the following equations in which  $A_f$  is the side area, and  $A_b$  is the base area of the fin,  $Q_{base}$  is the heat transfer to fin from the fin base, and  $T_b$  is the base temperature.

$$\eta_{fin} = \frac{Q_{base}}{h A_f (T_b - T_\infty)} \quad (7)$$

$$\epsilon = \frac{Q_{base}}{h A_b (T_b - T_\infty)} \quad (8)$$

In the above equations,  $h$  is the convective heat transfer coefficient, which can be calculated as follows:

$$h = \left( \frac{Q_{ave}}{A_s (T_{s,ave} - T_\infty)} \right) \quad (9)$$

where  $A_s$  is the surrounding area of the fin,  $T_{s,ave}$  is the average surface temperature of the fin and  $Q_{ave}$  is the average heat transfer to the fin, which equals to  $Q_{base}$ .

### 2.1 Problem definition and method of solution

In this research, the incompressible and three-dimensional flow inside the channel, including the porous fin of sintered 0.6 mm (fine grain) and 1.7 mm (coarse grain) balls made of copper, aluminum, and steel were studied. The characteristics of the fine-grain fins are shown in Fig. 1. In this case, the effect of two types of boundary conditions was investigated for the fin base. In the first case, the constant temperature and in the second case, the constant flux boundary conditions were considered at the base of the fin. The inlet boundary condition was obtained from the free flow condition, and

the outlet boundary condition was extrapolated from the inside solution zone.

In the numerical simulations, thermophysical properties for the solid phase of the porous medium was assumed to be uniform which leads to an easy and high-speed solution, but the accuracy will be lost a little with large temperature gradient changes. After defining the problem, the thermal behavior of the different materials used in the fin was compared. Other conditions of the problem are given in Table 1.

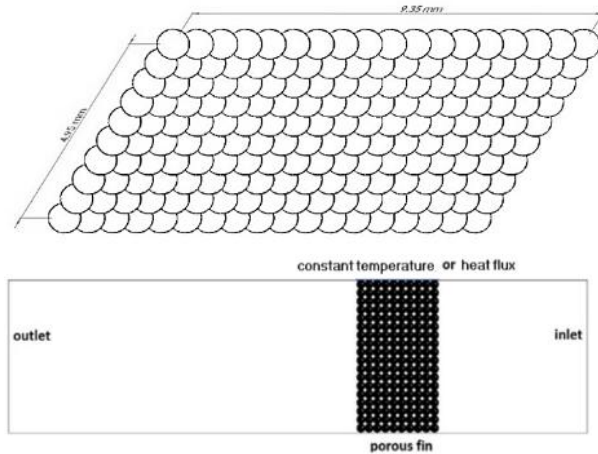


Figure 1. Schematic of boundary conditions, dimension, and fin

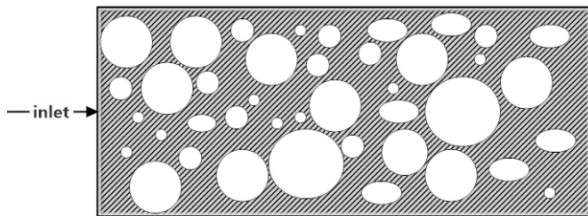


Figure 2. A real view of a simple, porous media

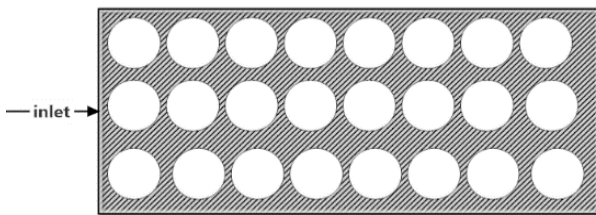


Figure 3. An assumed view of an engineered porous media

Table 1. Surface and volume analysis of solid and porous fin

type	Small size	Large size
Porosity volume	20.80	128.28
Porosity surface area	181.08	425.92
Rigid volume	33.88	230.78
Rigid surface area	131.81	249
Percentage in volume	-38.60	-55.56
Percentage in surface	37.38	171.05

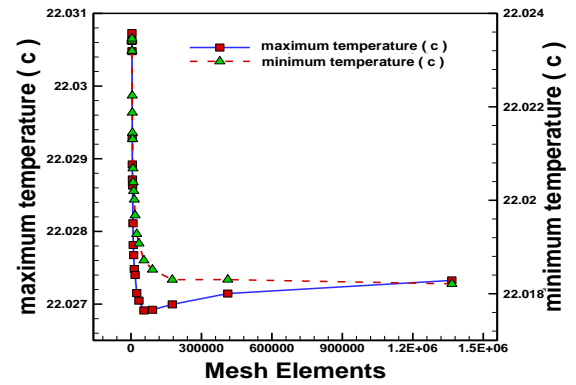


Figure 4. Grid independency for minimum and maximum temperature on the fin surface

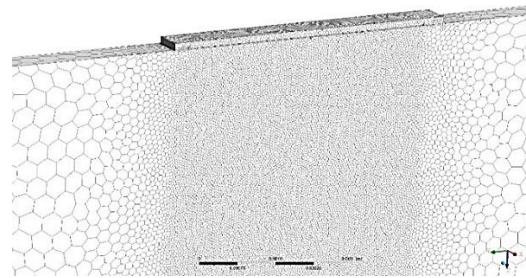


Figure 5. Final selected mesh

Regarding the numerical solution method, the SIMPLE algorithm was employed to couple the pressure and velocities. The second-order upwind scheme was applied to discretize the momentum, energy, turbulent kinetic energy, and turbulent energy dissipation equations. The convergence criterion of mass conservation equation was defined  $10^{-5}$  which is obtained from the residuals of continuity equation (velocity gradients for incompressible flow), and the convergence criterion of mass conservation equation is  $10^{-6}$  which was obtained from the residuals of temperature in each cell.

### 2.2 Surface analysis of the porous material

There are some assumptions about porous environments. Fig. 2, which is a real example of many porous environments, have a narrow passage in some areas and larger passages in other areas. This makes the solution of the equations and expansion of mathematical equations more difficult in these environments. In the coarse-grained fin, these values are much better; so that, despite a 55.5% reduction in fin volume, it increases the lateral surface about 171%. Therefore, the construction of such a porous fin is recommended in the ball with a larger diameter.

### 3. Mesh accuracy

In each numerical study associated with the generation of the network, one of the most important reports is the accuracy and independence of the network. For this purpose, in Fig. 4, the effect of changing the number and size of the network on the minimum and maximum temperature on the fin surface is expressed. As can be seen

from this diagram, there are no modifications in the assumptions and referred to an engineered porous environment, as shown in Fig. 3., in maximum and minimum temperatures after 400,000, so this number can be selected. Also, in this research, the developed polyhedral network has been used as a network. The most important features of this network type could be referred to its optimal structure. The network is based on an unstructured triangular based optimization algorithm. In the analysis of simultaneous conductive and convective heat transfer, network size is important, especially in determining the fluid temperature in the vicinity of the object. The selected sample of the network is shown in Fig. 5.

**Table 2. Conditions of the problem solution**

Type	Small size		Large size	
	Constant temperature	Heat flux	Constant temperature	Heat flux
Inlet velocity	0.00655	0.00655	0.0114	0.0114
Base temperature	450	-	450	-
Inlet temperature	289.17	289.17	300	300
Heat flux	-	14650	-	31730

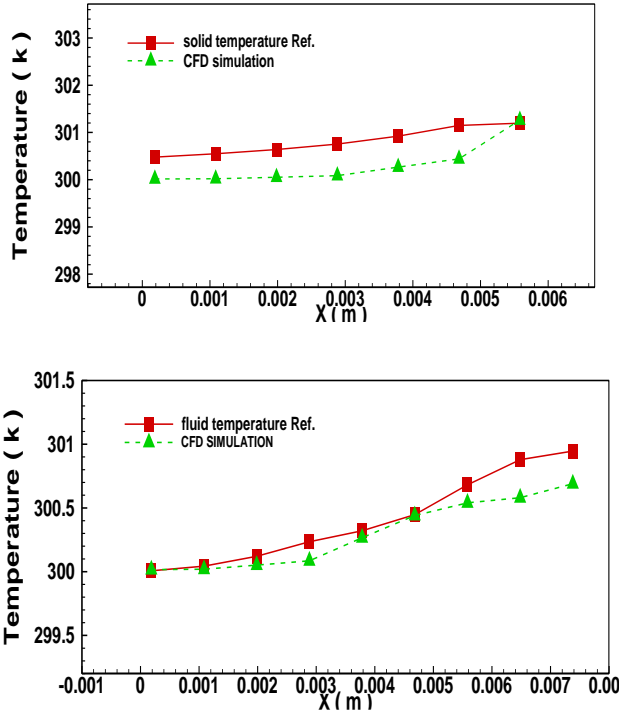


**Figure 6.** Validation for temperature distribution in (a) the fin, (b) the flow near the fin for 0.6 mm diameter spheres

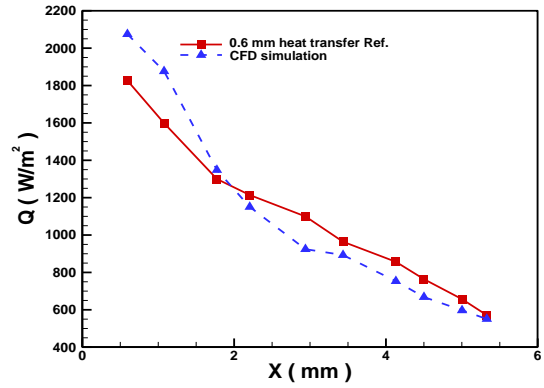


**Figure 7.** Validation of the heat transfer rate for 0.6 mm sphered fin and comparing the results with those of Ref. [13].

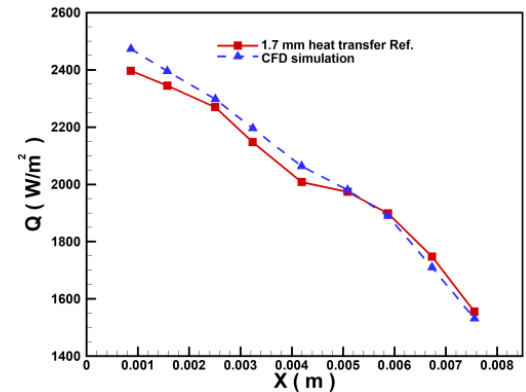


**Figure 8.** Validation of heat transfer rate for 1.7 mm sphered fin and comparing the results with those of Ref. [13].

#### 4. Validation of solution

All numerical studies require the validation and evaluation of output data. For this purpose, the data of the temperature distribution in solid body and fluid, as well as heat transfer and pressure drop, were investigated in accordance with the reference [18]. As shown in Fig. 6, the calculated fluid temperature (Fig. 6 (b)) is very close to the reference temperature of the fluid (about 1%) and the calculated surface temperature (Fig. 6 (a)), has a good accuracy of about 2.5% along the width of the fin (flow direction). The reason is the higher conductive heat transfer in Figs. 7 and 8. The heat transfer rate along the width of the fin (in the flow direction) is calculated for the fine-grain and coarse-grain fins and compared with the results of reference [18]. The results indicate the high accuracy of heat transfer rate calculations. As shown in this diagram, the heat transfer rate along the width of the fin (flow direction) is reduced. The reason for this decrease could be explained by the fact that at low velocities, the temperature and hydrodynamic boundary layers are thick. Therefore, the contribution of conductive heat transfer in the balls is higher compared to the convective heat transfer.

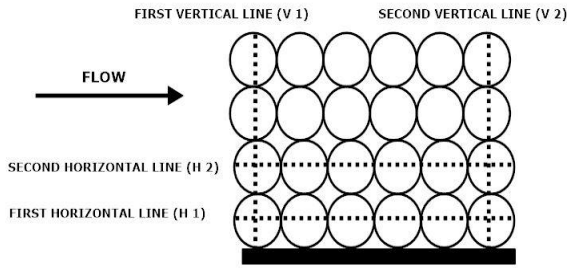


Figure 9. Defined lines for results comparison.

The rate was compared to the convection at low velocities, which increases the surface temperature relative to the fluid.

By moving along the fin widths, due to the greater contact of the balls, the contribution of the conductive heat transfer would increase, and the convective heat transfer would be reduced. In order to accurately determine the heat transfer values and also to temperature distribution in the case of the 4-contact connection, as in Fig. 9, reference lines are considered for calculation of the temperature and heat transfer for all modes of calculation.

These lines for horizontal mode are located in the first and second rows of the balls and for the vertical case, are located on the first and last rows of the balls. In this study, the heat transfer, the temperature distribution, and pressure drop in the 4-contact connection and also the material of balls under different thermal conditions of the base were investigated. More clearly, the heat transfer in the 4-contact mode was studied for three materials of steel, aluminum, copper under conditions of constant temperature and constant thermal flux for the fin base and two different diameters of the balls (0.6 and 1.7 mm). In all of these conditions, the flow boundary conditions were considered uniformly and in accordance with Table 1, so that, a comparison could be made between the performance of different materials from the heat transfer point of view. The results are presented as comparative graphs between different modes, and the conclusions were drawn based on these graphs.

### 5. Results and discussion

#### 5.1 The fine-grain fin with constant temperature boundary condition

According to the Fourier law, one of the effective factors in heat transfer is the thermal conductivity coefficient. This coefficient expresses the resistance of each body against the heat transfer. For the larger values of this coefficient and the lower resistance to the heat transfer, first, the body has better thermal conductivity, and second, the heat is transferred in the body in a shorter time. On the other hand, reduction in this coefficient increases the thermal resistance, and more time is required for reaching the thermal equilibrium. Accordingly, as shown in Fig. 10, it is observed that the temperature increases along the horizontal lines (along with the

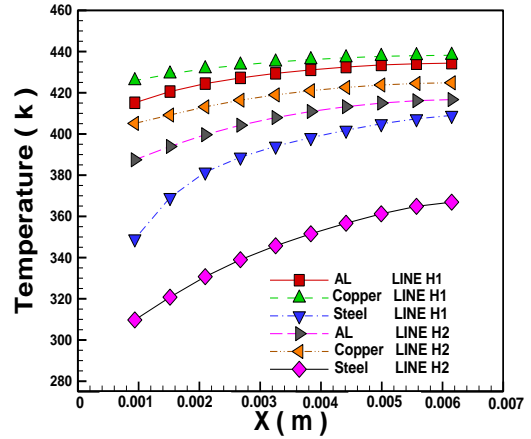


Figure 10. Temperature distribution on horizontal lines in flow direction for 0.6mm fin with constant temperature in the base.

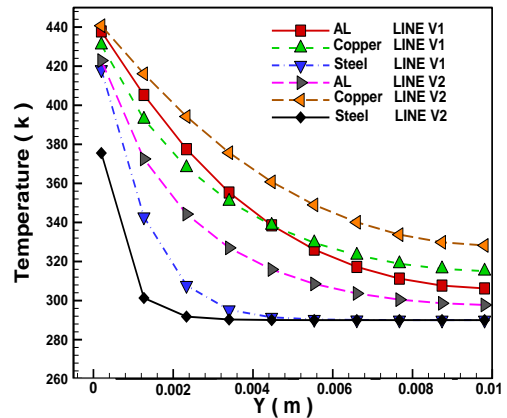
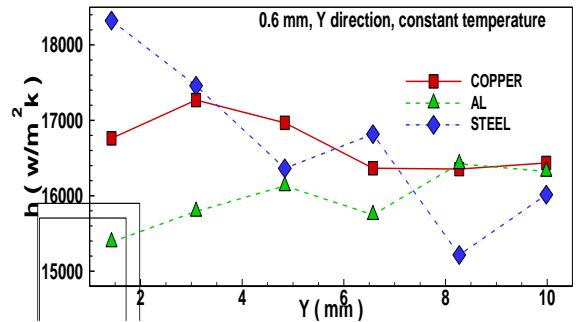
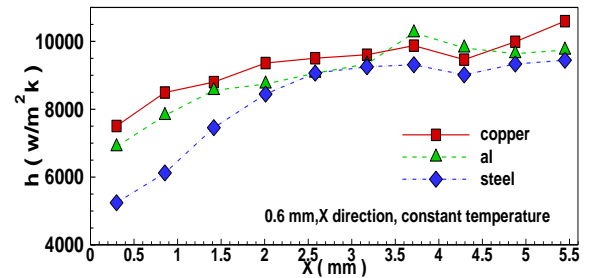


Figure 11. Temperature distribution on vertical lines for 0.6mm fin with constant temperature in the base.



(a)



(b)

Figure 12. heat transfer coefficient in vertical (a) and horizontal (b) for 0.6 mm sphere diameter and constant temperature in the base

current). The reason is that the temperature of the fluid flow through the fin increases and consequently, the transfer decreases, and also, due to the increased contact of the balls, the conductive heat transfer increased. As it is obvious, in contrast to the aluminum and copper, steel has a great difference both in the temperature values and growth manner, particularly for the second row. The reason for this difference is the difference in the thermal conductivity of steel with copper and aluminum. According to this diagram, the temperature variations in the horizontal direction of the fin is the lowest for the copper and is the highest for the steel. The reason is the higher conductivity coefficient of the copper, which increases the conductive heat transfer rate even in the initial balls, and the temperature of the balls increases near the edge of the collision. Interestingly, even in the first row near the base, the temperature of the steel fin has dropped compared to the copper and aluminum fin temperature in the second row. The reason is due to the lower conductivity.

In Fig. 11, the temperature distribution is shown for the first and the last vertical row. The aforementioned discussion is true for the temperature distribution in the vertical rows. The only difference is that by increasing the distance from the base of the fin, the surface temperature decreases, which is obvious. Here, the steel behavior is different for both lines compared to two other materials. In the steel, the temperature drops very quickly and reaches the ambient temperature, where the effective fin length is approximately 4.5 mm (7.5 times the diameter of a ball). As shown in this figure, the temperature decreases with increasing the length. Here, as in the previous section, the steel has a very distinct behavior compared to other metals. As it is obvious from the diagram, copper and aluminum have more uniform temperature variations along the fin, which is an advantage. It is also figured out that the copper has a higher surface temperature; therefore, the difference in the temperature of the fluid and the surface in the copper is higher than that of the aluminum, and the higher heat transfer rate occurred. Therefore, for a fin with constant temperature boundary condition at the base, the choice of copper, in addition to the more uniform distribution of heat, would lead to an increase in the heat transfer rate. In Fig. 12, the convective heat transfer coefficient in the direction perpendicular to the flow is shown for 0.6 mm fins in constant temperature, along the width. The reason for this is the presence of vortices behind the balls and intensifying the flow turbulence due to the roughness created in the direction of flow. However, in the perpendicular direction (along the fin), this trend is different and unconventional. It should be mentioned that the behavior of the steel near the base and the collision edge of the flow is different; however, it is the same at the end. As it is obvious, increasing the distance in the flow for them, when used as a fin, these metals could distribute the temperature almost uniformly throughout their length.

## 5.2 The fine-grain fin with constant flux boundary condition

The thermal flux applied in accordance with Table 2 is another part of this study. The constant thermal flux has been applied more than the constant temperature boundary condition in real cases. In order to create a constant temperature boundary condition in the body, only processes in which constant temperature can be generated, such as boiling and condensation processes, can be used.

On the other hand, the production of such processes is very difficult. All of these factors make the constant flux boundary condition more applicable. In Fig. 13, the temperature distribution diagram for constant heat flux is shown for the horizontal row of the balls along the flow direction. In this section, steel also has different behavior.

It is observed that for aluminum and copper, there is no significant difference in the temperature distribution over horizontal lines along with the flow, while there is a huge difference between the temperature of the first and second row of the steel fins. In Fig. 14, the temperature distribution is shown for the first and last vertical line (perpendicular to the flow direction). There is also no significant difference between the temperature distribution of copper and aluminum in this direction, and all the fins reach the ambient temperature at the end with a small amount of difference. With respect to Figs. 13 and 14, and also the slight difference in temperature distribution between copper and aluminum fins, and due to the lower production cost of aluminum fin compared to the copper in this case (constant flux at the base), aluminum is the best choice for the fin. For the steel, the effective length is also obtained at 4.5 mm. In Fig. 15, the temperature contour is determined for two states of constant flux and constant temperature for the steel. As it can be seen, in the constant temperature at the base of the steel fin, the temperature variation occurs in the smaller area of the fin, while this region is the biggest for copper fin, and the fluid passing from the copper becomes is warmer.

Furthermore, the white area of the fin for the steel and aluminum is a region that does not actually participate in the heat transfer and could be ignored. This area only increases the consumption of the material. In Fig. 16, for a fin with 0.6 mm diameter balls in the constant flux boundary conditions at the base, the convective heat transfer coefficient for the three different materials was calculated and compared.

The same points as in the previous figure are also observed here, with the difference that the thermal behaviour of the aluminium and copper fin are the same, and it can be said that by increasing the distance from the base of the fin, the heat transfer coefficient for these two materials is reduced, however, the heat transfer coefficient of the steel, which is the lowest in the perpendicular direction, increases with increasing the distance from the base. Therefore, in this case, due to its cost-effectiveness, the aluminum material is preferred.

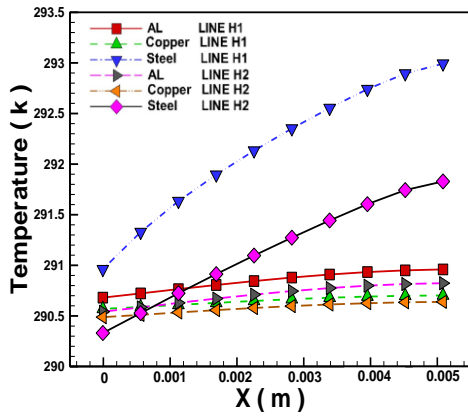


Figure 13. Temperature distribution on horizontal lines in flow direction for 0.6mm fin with constant heat flux in the base.

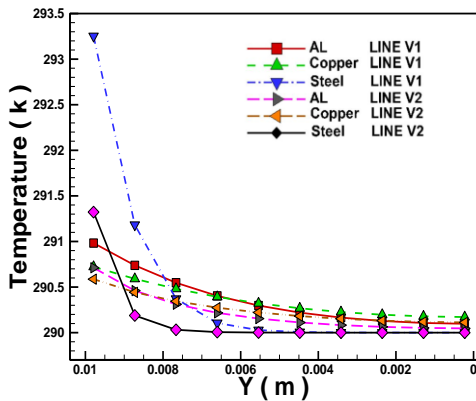


Figure 14. Temperature distribution on vertical lines for 0.6mm fin with constant heat flux in the base.

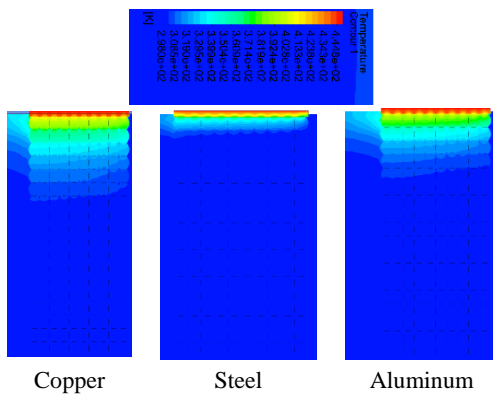
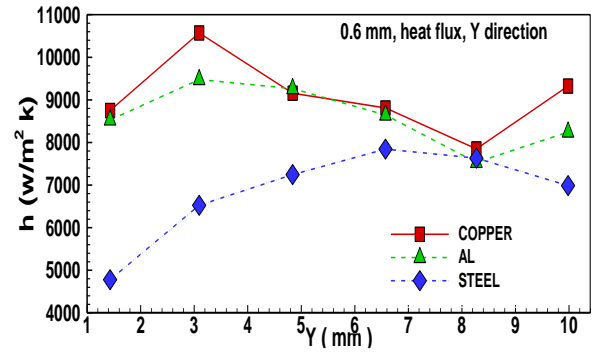


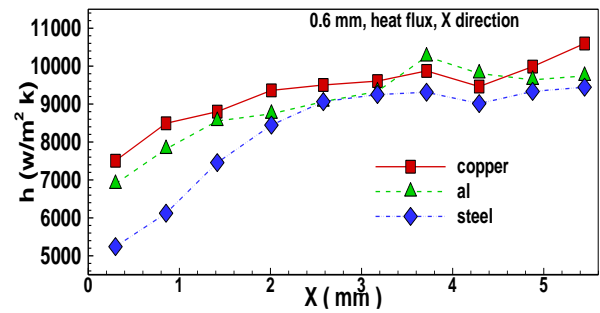
Figure 15. Temperature contour for three material with constant heat flux in the base.

### 5.3 The coarse-grain fin with constant temperature boundary condition

In this section, the thermal performance of the fin with a 1.7 mm balls with different material is studied. The temperature distribution is indicated in Figures 17 and 18. The results show that for horizontal lines (in line with flow), the temperature distribution slowly increases, as expected. Here, different behavior in values of growth of the temperature in the steel balls are seen. Also, in Fig. 18, the temperature distribution can be observed in a vertical direction (perpendicular to the flow direction).



(a)



(b)

Figure 16. heat transfer coefficient in vertical (a) and horizontal (b) for 0.6 mm sphere diameter and constant heat flux in base.

The behavior of the copper and aluminum fins are different, and with respect to the better thermal performance of copper (uniform distribution and higher temperature difference with fluid), for this condition (fixed base temperature), copper is selected.

The steel fin has the worst thermal performance due to the lack of uniformity and the lower temperature difference with fluid. So that only a few rows of balls perform heat transfer. In this case, the effective length of the steel fin can be considered to be 4.5 mm (about three rows of balls), and the rest will be ineffective in heat transfer. Compared to the constant temperature of Fig. 15 for copper and aluminum, the pale (low temperature) region in the constant flux is somewhat wider than the constant temperature. In Figure 19, the temperature contour is shown in a constant flux at the base for three different materials.

In Fig. 20, the heat transfer coefficient is calculated for the constant temperature boundary condition at the base of the fin with balls of 1.7 mm diameter for three different materials. The heat transfer coefficient increases with increasing distance from the edge of the attack along the flow. However, along the perpendicular direction, the heat transfer coefficient increases with increasing distance from the base for both aluminum and copper, in contrary to the fine grain fin, but decreases for the steel. Therefore, it is observed that with increasing the diameter of the balls, the behavior of the heat transfer coefficient varies in the perpendicular direction of the flow. Since the transferred

heat flux between the rows depends on the contact area of the balls with the flow, as well as the contact surface of the balls with each other, prediction and explanation of such behavior is complicated.

5.4 The coarse-grain fin with constant flux boundary condition

In Figures 21 and 22, the thermal behavior of the fin with a 1.7 mm ball in the constant thermal flux condition with different materials are shown. As it was expected, the temperature variation of the steel is steeper compared to other metals, so that the heat transfer occurs only in the 4.5 mm distance near the base (about three balls). Due to these two figures, thermal behavior of copper and aluminum is close to each other (not as much as a fine-grain fin), and the choice of aluminum is more cost effective in this situation. These results, compared to the results of a fine-grained fin, show that, with increasing the diameter of the balls and coarser grains, the thermal behavior of the aluminum is departing from the copper, and in higher diameters, copper may excel the aluminum from the heat transfer point of view. In Fig. 23, the convective heat transfer coefficient along the flow and perpendicular to the flow is shown for 1.7 mm ball with a constant flux at the base of the fin. In this case, there are no apparent changes for the heat transfer coefficient along with the flow. But for the steel, increasing the distance from the edge of the attack increases the convective heat transfer coefficient. However, the behavior of the convective heat transfer coefficient in the perpendicular direction of the flow is similar to figure 20 by increasing the distance from the base of the fin, with the constant temperature constant in the base. According to these two graphs it is also clear that as the diameter of the balls increases, the thermal heat transfer behavior of copper is superior to that of aluminum. Thus applying steel as the fin material is not suitable for both coarse- and fine- grain fins with different boundary conditions. Utilizing copper as fin material is more appropriate with constant heat flux compared with a constant temperature. For coarse-grain fin with aluminum material, the boundary condition of the base is not important for fin effectiveness. However, using constant temperature as the base condition of fine-grain aluminum fins would lead to higher effectiveness compared to constant heat flux. The efficiency of both coarse- and fine-grain fins is higher for constant heat flux compared to constant temperature as a boundary condition of the base. Fin with copper material has the highest efficiency compared to other materials in all states.

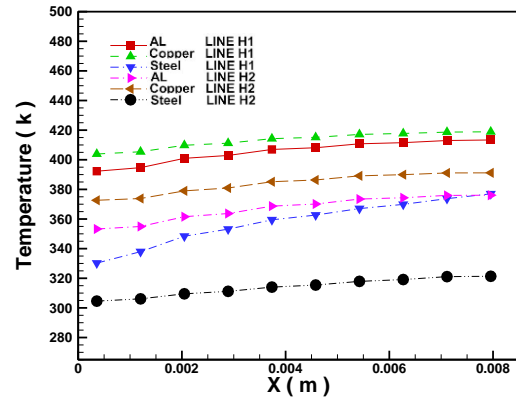


Figure 17. Temperature distribution on horizontal lines in flow direction for 1.7 mm fin with constant temperature in the base

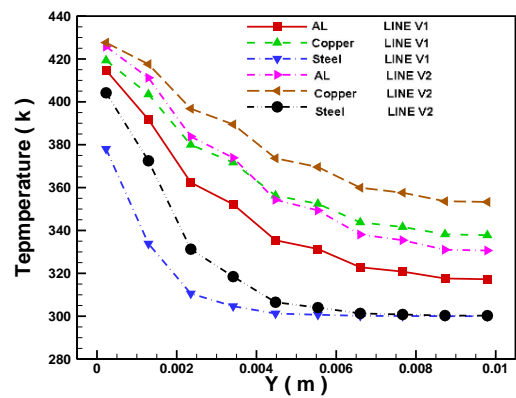


Figure 18. Temperature distribution on vertical lines for 1.7 mm fin with constant temperature in the base

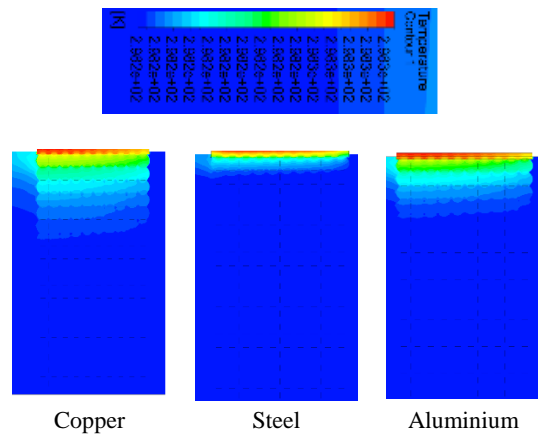


Figure 19. Temperature contour for three material with constant heat flux in the base

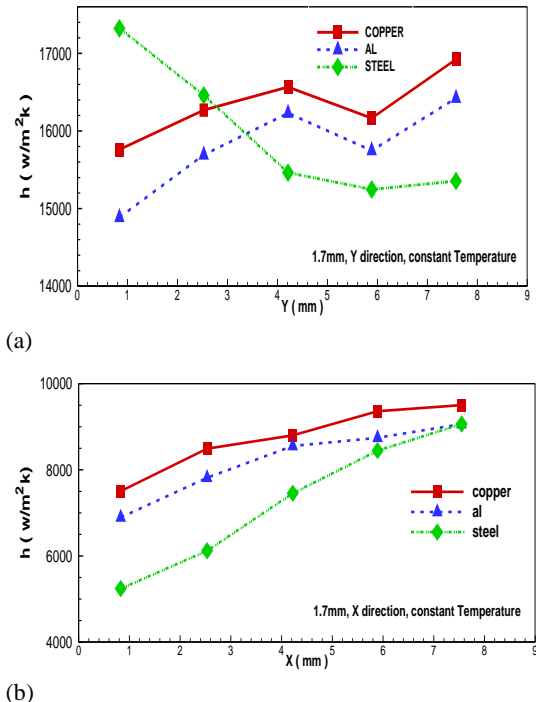


Figure 20. heat transfer coefficient in (a) vertical and (b) horizontal, for 1.7 mm sphere diameter and constant temperature at the base.

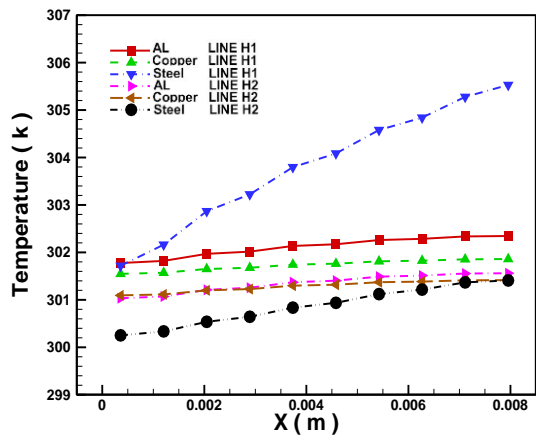


Figure 21. Temperature distribution on horizontal lines in flow direction for 1.7 mm fin with constant heat flux in the base

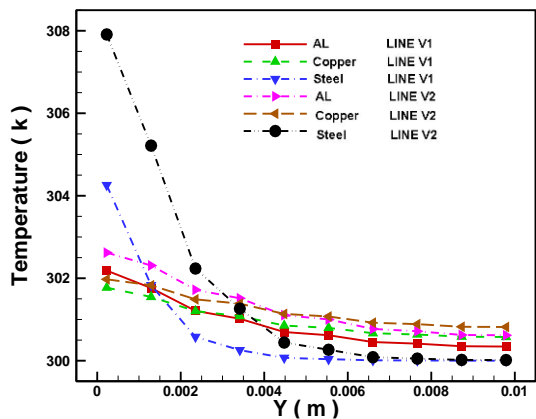


Figure 22. Temperature distribution on vertical lines for 1.7 mm fin with constant heat flux in the base.

5.3 Efficiency and effectiveness analysis

In order to evaluate the heat transfer performance of fin with different material and boundary conditions for fine- and coarse-grain, the effectiveness and efficiency were obtained from Eqs. (8) and (9) and are presented in Table 3. As it is known, fin with effectiveness below two is not preferable to apply. Thus applying steel as the fin material is not suitable for both coarse- and fine- grain fins with different boundary conditions. Utilizing copper as fin material is more appropriate with constant heat flux compared to a constant temperature. For coarse-grain fin with aluminum material, the boundary condition of the base is not important for fin effectiveness. However, using constant temperature as the base condition of fine-grain aluminum fins would lead to higher effectiveness compared to constant heat flux. The efficiency of both coarse- and fine-grain fins is higher for constant heat flux compared to constant temperature as a boundary condition of the base. Fin with copper material has the highest efficiency compared to other materials in all states.

Table 3. Effectiveness and efficiency of the fin with different material and boundary condition for fine- and coarse-grain

	effectiveness			effectiveness		
	Cu	Al	Steel	Cu	Al	Steel
Ball dia. 1.7 mm						
Constant heat flux	3.04	2.1	1.03	92.84	84.56	66.64
Constant temp	2.41	2.1	1.88	89.55	81.74	58.87
Ball dia. 0.6 mm						
Constant heat flux	2.85	1.84	1.55	97.15	91.77	67.84
Constant temp	2.62	2.29	2.00	94.23	87.57	67.88

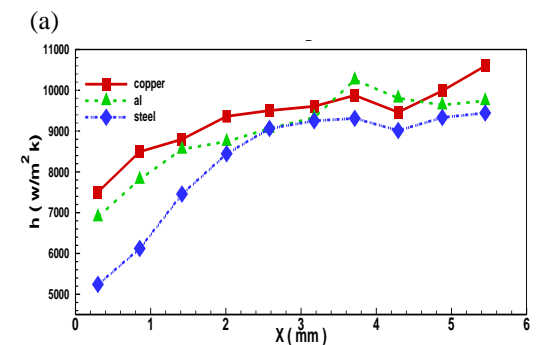
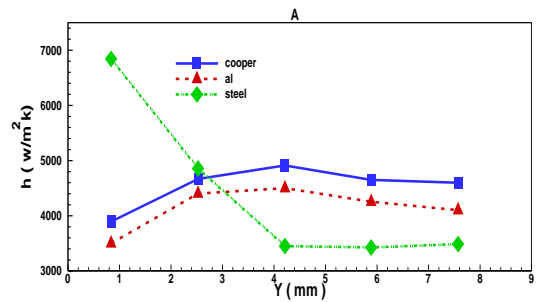


Figure 23. heat transfer coefficient in vertical (a) and horizontal (b) for 1.7 mm sphere diameter and constant heat flux in the base.

## 6. Conclusion

In this study, the behavior of heat transfer in two sets of sintered balls of copper, aluminum, and steel with different dimensions of 0.6 and 1.7 mm was investigated. In order to determine the thermal behavior of the fins, two conditions were considered; the constant temperature and the constant flux. Important results are listed below:

In an engineered porous fin with constant flux at the base and small diameter balls, due to the closeness of the thermal performance of copper and aluminum, the suitable and cost-effectiveness material is aluminum.

However, for higher diameters with the constant flux at the base, the heat transfer performance of the balls, the copper is diverted from aluminum and gets better. With constant temperature and constant flux boundary condition for all the diameters, the copper has a better thermal performance.

Steel has no advantage in selection of material for the fin balls; and in all cases, only 4.5 mm of its length was involved in heat transfer.

## Nomenclature

A	area $\text{m}^2$
E	Module elasticity $\text{N/m}^2$
C	Thermal capacity $\text{J/K}$
g	gravity $\text{m/s}^2$
h	Heat transfer coefficient $\text{W/m}^2 \cdot \text{K}$
K	Conduction heat transfer coefficient $\text{W/m}^2 \cdot \text{K}$
L	length $\text{m}$
m	mass $\text{kg}$
q	Heat flux, $w$
T	Temperature, $k$
U	X velocity $\text{m/s}$
V	velocity $y$ $\text{m/s}$

## References

- [1] Y. A. Cengel, M. A. Boles, M. Kanoglu, Thermodynamics: an engineering approach. 5th edition, McGraw-Hill New York, (2011).
- [2] A. Bejan, A. M. Morega, Optimal arrays of pin fins and plate fins in laminar forced convection. *Journal of Heat Transfer*, 115(1), 75-81, (1993).
- [3] R. A. Wirtz, A semi-empirical model for porous media heat exchanger design. *ASME-PUBLICATIONS-HTD*, 349, 155-162, (1997).
- [4] T. M. Jeng, S.C. Tzeng, Numerical study of confined slot jet impinging on porous metallic foam heat sink. *International Journal of Heat and Mass Transfer*, 48(23), 4685-4694, (2005).
- [5] J. Ma, Y. Sun, B. Li, Simulation of combined conductive, convective and radiative heat transfer in moving irregular porous fins by spectral element method, *International Journal of Thermal Sciences*, 118, 475-487, (2017).
- [6] H. Chen, J. Ma, H. Liu, Least square spectral collocation method for nonlinear heat transfer in moving porous plate with convective and radiative boundary conditions, *International Journal of Thermal Sciences*, 132, 335-343, (2018).
- [7] J. Ma, Y. Sun, B. Li, Hao Chen, Spectral collocation method for radiative-conductive porous fin with temperature dependent properties, *Energy Conversion and Management*, 111, 279-288, (2016).
- [8] M. Hamdan, and A.N. Moh'd, The use of porous fins for heat transfer augmentation in parallel-plate channels. *Transport in porous media*, 84(2), 409-420, (2010).
- [9] L. Chuan, X-D. Wang, T-H. Wang, W-M. Yan, Fluid flow and heat transfer in microchannel heat sink based on porous fin design concept. *International Communications in Heat and Mass Transfer*, 65, 52-57, (2015).
- [10] G. Lu, J. Zhao, L. Lin, X-D. Wang, W-M. Yan, A new scheme for reducing pressure drop and thermal resistance simultaneously in microchannel heat sinks with wavy porous fins. *International Journal of Heat and Mass Transfer*, 111, 1071-1078, (2017).
- [11] K.S. Ong, Heat spreading and heat transfer coefficient with fin heat sink. *Applied Thermal Engineering*, 112, 1638-1647, (2017).
- [12] M. Lindstedt, R. Karvinen, Conjugated heat transfer from a uniformly heated plate and a plate fin with uniform base heat flux. *International Journal of Heat and Mass Transfer*, 107, 89-95, (2017).
- [13] A. Bejan, Entropy generation minimization: The new thermodynamics of finite size devices and finite time processes. *Journal of Applied Physics*, 79(3), 1191-1218, (1996).
- [14] L. Chen, Constructal entropy generation rate minimization for cylindrical pin-fin heat sinks. *International Journal of Thermal Sciences*, 111, 168-174, (2017).
- [15] M. Mesgarpour, A. Heydari, S. Saedodin, Numerical analysis of heat transfer and fluid flow in the bundle of porous tapered fins, *International Journal of Thermal Sciences*, 135, 398-409, (2019).
- [16] P.X. Jiang, M. Li, T.J. Lu, L. Yu, Z.P. Ren, Experimental research on convection heat transfer in sintered porous plate channels. *International Journal of Heat and Mass Transfer*, 47, 2085-2096, (2004).
- [17] P.X. Jiang, M. Li, Y.C. Ma, Z.P. Ren, Boundary conditions and wall effect for forced

- convection heat transfer in sintered porous plate channels, *International Journal of Heat and Mass Transfer*, 47, 2073-2083, (2004).
- [18] PX. Jiang, X.C. Lu, Numerical simulation of fluid flow and convection heat transfer in sintered porous plate channels. *International Journal of Heat and Mass Transfer*. 49(9), 1685-95, (2006).
- [19] M. Mesgarpour, A. Heydari, S. Saedodin, " Investigating the effect of connection type of a sintered porous fin through a channel on heat transfer and fluid flow", *Journal of Thermal Analysis and Calorimetry*, (Doi: 10.1007/s10973-018-7356-y).
- [20] A. Bejan, *Designed Porous Media*, in *Emerging Technologies and Techniques in Porous Media*, Springer, 337-349, (2004).
- [21] C. K. Ho, S.W. Webb, *Gas transport in porous media*, Springer, (2006).
- [22] D. A. Nield, A. Bejan, *Convection in porous media*. Springer, (2006).
- [23] FLUENT User's Guide, Release 6.1. FLUENT Inc., Lebanon, (2001).
- [24] P. M. Adler, *Porous media: geometry and transports*, Butterworth-Heinemann, (1992).
- [25] J. Bear, M.Y. Corapcioglu, *Fundamentals of transport phenomena in porous media*, M. Nijhoff, (1984).
- [26] J. B. Keller, *Flow in random porous media*. *Transport in Porous Media*,. 43(3), 395-406, (2001).
- [27] K. Vafai, *Handbook of porous media*, Crc Press, (2009).